

Author(s): Benkreira, H.

Title: Dynamic wetting in metering and pre-metered roll coating
Publication year: 2002

Journal title: Chemical Engineering Science

ISSN: 0009-2509

Publisher: Elsevier Ltd.

Publisher's site: *http://www.sciencedirect.com*

Link to original published version: *http://dx.doi.org/10.1016/S0009-2509(02)00175-6*

# DYNAMIC WETTING IN METERING AND PRE-METERED FORWARD ROLL COATING

H. Benkreira

Chemical Engineering, University of Bradford, Bradford BD7 1 DP, UK,

E-mail H. Benkreira@bradford.ac.uk

***Abstract**: This experimental study of dynamic wetting in metering and pre-metered forward roll coating shows that the dimensionless applicator flow rate $\lambda_{A,}$ is the key parameter as it defines whether dynamic failure occurs by air entrainment ($\lambda_A > \lambda_{A,\,trans}$) or cascade ($\lambda_A < \lambda_{A,\,trans}$). $\lambda_{A,\,trans}$ is the flow rate when the regime switches from metering to pre-metered and $\lambda_{A,\,min}$, the minimum flow rate in the pre-metered regime. When Ca was varied in the range 0.2→5, $\lambda_{A,\,trans}$ and $\lambda_{A,\,min}$ were in the range 1.40→1.29 and 1.20→1.18 respectively. These values compare very well with theoretical predictions. The air entrainment speeds $V^*_M$ were found to be similar to the corresponding speeds $V^*_{plunging}$, measured in plunging tape flow but the cascade speeds $V^{**}_M$ can be smaller or larger depending on $\lambda_A$. This led to exploring hydrodynamic assistance and drawing an analogy with curtain coating, which was supported by the data. It was also observed that cascade occurred in the pre-metered regime because the dynamic wetting line $X_D$, moves near the minimum gap position just as in reverse roll coating. Indeed the cascade speeds conform to correlations developed for reverse roll coating. Finally the study gives data on $X_D$, and compares them with theoretical predictions. The agreement in this case is only qualitative and this points to deficiencies in current modeling of the dynamic wetting region.*

***Key words**: Air Entrainment, Coating, Dynamic Wetting, Films, Fluid Mechanics, Hydrodynamics.*

## 1. INTRODUCTION

Forward roll coating is an important industrial coating operation and a model coating flow much researched theoretically and experimentally (Kistler & Schweizer, 1997). As shown in Figure 1, it consists of an applicator roller rotating at speed $V_A$ and supplying a feed film $H_A$ to a metering nip $H_0$ , and a metering roller driving a substrate at speed $V_M$. The coated films are the two films, which form at exit of the nip. These films are not always uniform; outside an operating window, they may be ribbed or entrain air. Ribbing is associated with surface instabilities, which occur at the separation meniscus where the two films form. This paper is concerned only with dynamic wetting, which occurs upstream at the dynamic wetting line, $X_D$. It is the failure of dynamic wetting that causes air to be entrained either as very fine or very large bubbles. Very fine bubbles air entrainment is observed most typically in the plunging tape flow, where above a critical speed, $V^*_{plunging}$, the dynamic wetting line changes from a straight line into a vvv-shaped line with tiny air bubbles detaching from the tips of the v-segments. This is now a classical observation reported first by Deryagin & Levi (1964) and later by many researchers including Burley & Kennedy (1976), Blake & Ruschak (1979), Gutoff & Kendrick (1982) and Cohu & Benkreira (1998). The data all show that for smooth substrates and zero wetting angle[1], $V^*_{plunging}$ is controlled essentially by viscosity. It is proportional to $\mu^{-0.67 \rightarrow -0.87}$ when $\mu < 0.5$ Pa.s and has an upper limit of about 0.1 m/s for fluids of $\mu \geq 0.5$ Pa.s. A typical and often quoted correlation is that due to Gutoff & Kendrick (1982):

$$V^*_{plunging} = 0.05\ \mu^{-0.67} \qquad (1.1)$$

[1] Substrate roughness (Buonoplane, Gutoff & Rimore, 1986) and non-zero wetting angles (Cohu & Benkreira, 1998) postpone air entrainment to significantly higher speeds.

Gutoff & Kendrick (1987) and Lee & Liu (1990) found similar air entrainment type and speeds in slide and slot coating respectively. The dynamic wetting regions in these flows are very similar to that in the plunging tape flow and this can explain these results. Burley (1992) went further and argued that the plunging tape air entrainment results are applicable to all coating flows. An examination of the data of Kistler (1984) shows this is not the case with curtain coating, which can operate 10 times faster before entraining air. Blake, Clarke & Ruschak (1994) attributed this difference to hydrodynamic effects, which in curtain coating assist wetting by pinning the dynamic wetting line. Effectively, the controlling parameter is the characteristic speed $U_i$ of the liquid curtain impinging on the wetting line. Both the magnitude and direction of $U_i$ in relation to the wetting line play a part. The experimental data of Yamamura, Suematsu, Kajiwara, & Adachi (2000) showed hydrodynamic assistance is greatest or $V^*_{curtain}$ is maximised, when the wetting line is located right beneath the impinging curtain. Blake *et al.* (1994) found that $V^*_{curtain,\,max}$ also correlates with viscosity but to a lesser extent than in the plunging tape flow:

$$V^*_{curtain,\max} = 2.46\ U_i^{0.66}\ \mu^{-0.17} \qquad (1.2)$$

This agrees with the argument that at critical conditions, the force dragging the wetting line must just balance the force pinning it, which equates according to Blake *et al.* (1994) to:

$$V^*_{curtain,\max} = 2.18\ U_i^{0.81}\ \mu^{-0.19} \qquad (1.3)$$

The question is then: is the plunging tape air-entrainment result applicable to forward roll coating or is there, under certain feeding conditions, hydrodynamic assistance of wetting? The answer to this query forms our first objective.

The second form of dynamic failure is the so-called cascade where large bubbles are *engulfed* in the coated film. Coyle, Macosko & Scriven (1990) first reported it in reverse roll coating and

explained it as the result of the breaking of the dynamic wetting line on the metering roller when it is near the minimum gap position, i.e. it is induced by the converging-diverging geometry of the nip between the two rollers, which *traps* the wetting line. Benkreira (2001) confirmed this mechanism by providing data, over a larger range of capillary numbers, on the movement of the dynamic wetting line position $X_D$ with metering roller speed up to dynamic wetting failure. The correlations of Coyle *et al.* (1990) and Benkreira (2001) for the onset of cascade[2], expressed in terms of the metering capillary number $Ca^{**}_M$ ($=\mu V^{**}_M/\sigma$) and the applicator capillary numbers $Ca_A$ ($=\mu V_A/\sigma$) and in agreement with one another are respectively:

$$Ca^{**}_M = 0.43\ Ca_A^{0.54} \qquad (1.4)$$

$$Ca^{**}_M = 0.41\ Ca_A^{0.69} \qquad (1.5)$$

Benkreira (2001) compared his cascade data with plunging tape air entrainment speeds and concluded that although the two forms of air entrainment are different, the applicator roller in reverse roll coating enables operation at higher metering roller speeds, i.e. it provides hydrodynamic assistance. Moreover, he found the data to conform to the above correlations (1.2) and (1.3), which describes hydrodynamic assistance in curtain coating albeit that the metering roller speeds are much lower. The second objective is then to assess if this is also the case in forward roll coating.

The third and final objective must be to study the mechanism(s) by which dynamic failure occur in forward roll coating by monitoring the movement of the dynamic wetting line as the metering roller speed is increased for various feed flow conditions. Is air entrainment by cascade or the vvv-type? Does it depend on whether the flow is operated in the metering or pre-metered mode?

[2] Throughout this text, superscript *refers to v-type air entrainment and ** to cascade.

By controlling the inlet feed to the coating gap, forward roll coating can be operated over a range of regimes as illustrated in Figure 2. This goes from the metering (flooded feed)– where $H_A/H_0>>1$ (~10), $X_D$ is far upstream and more liquid is delivered to the coater that can actually pass through the nip to the extreme pre-metered regime (meniscus) – where $H_A/H_0 <<1$ (~0.1), $X_D$ is right inside the nip and all the liquid delivered, $Q_A$ ($=V_AH_A$) passes through the nip. For the flooded feed metering flow situation, Benkreira, Edwards & Wilkinson, (1981a) tested a series of fluids of different viscosities over a range of roller speeds, speed ratios and gaps and found $Q_N$, the net flow rate through the nip to be constant and about 1/3% larger than the drag flow $Q_D=1/2(V_A+V_M)\ H_0$. The actual measurements gave the dimensionless net flow $\lambda_N$ ($=Q_N/Q_D$)=1.31 with a standard deviation of 0.4%. Benkreira, Edwards & Wilkinson, (1981b) confirmed this result theoretically using a simple lubrication analysis. Coyle, Macosko & Scriven (1986) approached the analysis more rigorously using finite elements calculations and found similar results; $\lambda_N$ varied from 1.33 to 1.29 as the average capillary number Ca ($=1/2(V_A+V_M)\mu/\sigma$) was increased from 0.01 to infinity for equal speeds. $\lambda_N$ insensitivity to roll speed ratio is reflected in that $\lambda_N$ was computed =1.23 for $V_M/V_A=0$ and $Ca=\infty$. Neither Benkreira *et al.* (1981) or Coyle *et al.* (1986) considered dynamic wetting and its failure, which should occur above a certain metering roller speed (their $X_D \rightarrow -\infty$ did not enter in the analysis). Chen and Higgins (1988) were probably the first to quantify how $X_D/H_0$ varies with Ca in forward roll coating with a controlled applicator feed $Q_A$, corresponding to a dimensionless feed flow rate $\lambda_A$ ($=Q_A/Q_D$). By restricting their analysis to no *run-back flow* (see Figure 2b), they could impose a fixed $\lambda_A$ at the inlet boundary. Then fixing at $X_D$ the contact angle and a slip length enables the computation of the shape of the bead at inlet all the way to the minimum gap position. Their

predictions however were limited to one value of $\lambda_A$=1.226 and for equal roller speeds which corresponds to the lubrication approximation solution of the flow with inlet pressure boundary condition, $P \rightarrow 0$ as $X_D \rightarrow -\infty$ and outlet boundary conditions, P=dP/dX=0 at the films split location. For this value of $\lambda_A$=1.226, they found that increasing the capillary number from 0.02 to 0.3 moves the wetting lines upstream of the nip from $60H_0$ to $90H_0$. Benjamin (1994) used essentially the same approach as Chen & Higgins (1988); he too restricted the analysis to no *run-back flow* but extended it to cases of controlled feed with a range of $\lambda_A$>1 and <1. He also subjected the results to a two-dimensional stability test. He found *regular turning points* in the prediction of $X_D/H_0$ vs. $\lambda_A$ and Ca, which split the solutions into stable and unstable types limited by a minimum $\lambda_{A,\,min}$ and a maximum $\lambda_{A,\,max}$. In the high capillary number range of interest to forward roll coating ($0.1<Ca<10$)[3], the stable coating window was found to be divided into six quality windows defined by the number of *gyres* present in the flow. The limiting $\lambda_{A,\,min}$ and $\lambda_{A,\,max}$ and corresponding $X_D/H_{o\,min}$ and $X_D/H_{o\,max}$ are shown in Figure 4 with the results of our study. For the range $Ca=0.1 \rightarrow 10$, $\lambda_{A,\,min} = 1.21 \rightarrow 1.18$ corresponds to the onset of dynamic failure by cascade and $\lambda_{A,\,max} = 1.31 \rightarrow 1.26$ defines the start of a transition regime which leads to metering flow. Carvalho & Scriven (1997) also carried out a finite elements model of the controlled feed flow but for the difficult conditions of $H_A/H_0$>1 where both metering and pre-metered flow could occur. They first pointed that some of the $\lambda_A$ values considered by Benjamin (1994) were not pre-metered, i.e. controlled feed, and interacted with the imposed inflow boundary condition. As there could be interaction between the feed conditions and the coating bead in their case study, Carvalho & Scriven (1997) did not impose a velocity profile at the inlet boundary; they used

[3] We are not concerned in this study with the extreme pre-metered meniscus coating regime for which Ca<0.01, $H_A/H_0 << 1$ and $\lambda_A << 1$ (see Gaskell *et al.*, 1995).

instead the so-called *free boundary condition* (see Papanastasiou, Malamataris & Ellwood, 1992). They were able to obtain flow states that extended to both metering and pre-metered flow situations. In particular they gave predictions of how $X_D/H_0$ varies with $\lambda_A$ in these flows and established that the transition from metering to pre-metered occurred near $\lambda_{A,\ trans}$ =1.33 when Ca=0.1. (Note that this $\lambda_{A,\ trans}$ is equivalent to Benjamin's (1994) $\lambda_{A,\ max}$). They did not give how $\lambda_{A,\ trans}$ varied with Ca but identified $\lambda_{A,\ min}$ =1.22 when Ca=0.1 as the minimum value below which two-dimensional steady states do not exist. This corresponds to the onset of cascade and is identical to the value found by Benjamin (1994) for the same Ca. At this condition, they found as Benjamin (1994) did, the dynamic wetting line positioned very near the minimum gap, i.e. $X_D$~0. The theoretical results of Chen & Higgins (1988), Benjamin (1994) and Carvalho & Scriven (1997) form a useful indicator of how the flow may behave in controlled feed situation and at the transition metering / pre-metered, they are not however backed by experimental data. All the three analyses make assumptions on the contact angle $\theta_D$ and the slip length, cannot account for non-hydrodynamic molecular effects and inherently disregard the vvv-type mode of dynamic failure, which a-priori should occur under certain operating conditions (when $\theta_D \rightarrow 180^0$). Also Carvalho & Scriven (1997) limited their predictions to the one value of Ca=0.1, Chen & Higgins (1988) to the one value of $\lambda_A$=1.226 and some of Benjamin's (1994) predictions were questioned by Carvalho & Scriven (1997). The third and final objective of this paper then becomes complementary to these studies: to verify the theoretical findings by providing data on the movement of $X_D$ up to dynamic failure (be it by cascade or vvv-type) as a function of Ca and $\lambda_A$ from the flooded feed regime, past the transition boundary and into the pre-metered regime with both $H_A/H_0$<1 and >1. It must be noted that the measurement of $X_D$ is a very difficult task (see

Benjamin, 1994) and the development of a reliable technique forms in itself an associated aim of this research.

## 2. EXPERIMENTAL SET-UP

The pilot coater is described in Figure 3 and consists of a solid steel frame holding two rollers, one on top of the other, separated by a gap. The bottom roller (the applicator roller) was made out of steel, chrome plated and polished and the top roller (the metering roller) of cast perpex polished to give maximum transparency. The rollers were 19 cm long x 20 cm diameter with ± 0.1 micron surface finish and an eccentricity not varying by more than ± 5 microns. Inverter controlled AC geared motors drove the rollers independently via a combination of timing pulleys and belts. Initial calibration of the inverters provided accurate control of the roller speeds (less than 0.1 m/min). The applicator roller was immersed in a rectangular trough and a scraper blade attached to a vernier metered the liquid film it carried at any speed. The ensuing film thickness was measured using a needle attached to a micrometer and a CCD camera linked to a PC. The image of the contact needle-fluid was magnified and the micrometer was turned until the needle just touched the surface of the film. The metering roller was wiped clean and dry by a plastic scraper to ensure the formation of a dynamic wetting line. The gaps between the rollers were set by placing shims accurate to ± 0.1 micron between the roller bearing blocks and checked using slip gauges.

The onset of vvv-type air entrainment or cascade was depicted visually from above the perspex-metering roller. The dynamic wetting region was observed by illuminating the gap and at a fixed applicator roll speed, the metering roll speed was gradually increased until the wetting line broke. In order to reduce experimental errors, each data point was repeated at least four times. In spite of

the relative crudeness of the experimental method, the discrepancies between individual and averaged speed data were always found to be less than ± 9%.

For the measurement of the dynamic contact line position, $X_D$, we focused directly above the perspex metering roller a CCD camera (Pulnix 765TM) coupled with a Canon macro lens (50mm, 1:3.5) and mounted on an accurately moveable x-y-z platform. The images taken were fed directly to a PC. The magnification of the images was determined using a photograph of a graticule placed in the nip between the rollers. The location of the centre axis of the nip as viewed from the camera was determined by marking a line on the applicator steel roller and aligning it at its upper most position. With both rollers stationary, an image was captured to give the position of the centre line. With the rollers rotating during the coating experiments, images were collected to measure the position of the wetting line $X_D$ with reference to this centre line. In the actual experiments, the gap, film thickness and applicator speeds were kept constant and the metering roller speeds increased in steps of 5m/min until air entrainment or cascade occurred. The metering roller speed was then fractionally reduced by about 0.1m/min below the critical speed.

During this experimental programme, five lubricating oils of viscosities 0.030, 0.050, 0.150, 0.230 and 0.310 Pa.s were tested at gaps of 0.25, 0.50, 0.75, 1.00 and 1.25 mm with the applicator roller speeds varying from 5 to 60 m/min in 5 m/min steps. The viscosities of the fluids were measured in a Brabender Rheotron Rheometer and found to be Newtonian. Their surface tensions were measured using the pendent drop method, and found to be 0.035 $Nm^{-1}$ ± 2%. For the flooded regime mode of operation, the thickness of the arriving feed films was always much larger than the gap. In the pre-metered mode of operation, the arriving feed film thickness could be larger, equal or smaller than the gap. For the purpose of comparison, the air entrainment in

plunging tape flow was also measured with the test liquids using our laboratory dip coater described previously (Cohu & Benkreira, 1998).

## 3. RESULTS AND DISCUSSION

As explained earlier, the critical parameter must be the dimensionless applicator feed flow rate $\lambda_A$ which describes the flow regime at entry. In the treatment of the data, inertia and gravity effects are ignored and the effects of fluid properties are lumped in the average capillary number Ca as is carried out in theoretical modelling. The 600 data points for the tested conditions in the range $1.15<\lambda_A<2.6$, $0.1<Ca<5$ with $0.6<H_A/H_0<1.4$ and larger (for the flooded feed regime) are mapped in Figure 4 and 5a,b in the guise of $\lambda_A=f$ (Ca) and $X_D/H_0=f$ ($\lambda_A$, Ca) to establish the transition metering / pre-metered regime and assess dynamic wetting and the mechanism leading to it failure in both regimes. These figures serve also as a basis for comparing the data with the theoretical predictions of Benjamin (1994), Carvalho & Scriven (1997) and Chen & Higgins (1988).

**3.1 Metering Regime**: The reference flow must be the flooded feed metering regime for which $Q_A>>Q_N$ corresponding to $\lambda_A>>1.31$ and $\lambda_N=1.31$, independently of Ca (see above Benkreira *et al.*, 1981 and Coyle *et al.*, 1986). In this situation, the measured position of the dynamic wetting line was well out of the nip (as shown in Figure 4), the liquid fell back and formed a lip on the applicator film and at the critical metering roller speed $V^*_M$ just prior to air entrainment the dynamic wetting line adopted the classical vvv-type shape. When these $V^*_M$ are compared with $V^*_{plunging}$ measured in the plunging tape flow with the same fluids, they are found to be identical as shown in Figure 7 (further discussion in section 3.4). Therefore, the plunging flow describes well dynamic wetting in the flooded forward roll coating regime.

**3.2 Transition Metering / Pre-metered**: Whilst keeping $H_A/H_0$ not much >1 (typically < 1.40), when $Q_A$ was reduced to the point where the liquid did not fall back on the applicator film, a rolling bank formed as in Figure 2b; $Q_A=Q_N$ and $\lambda_A=\lambda_N$ ; and we were at the transition metering /pre-metered which we measured to be $\lambda_{A,\ trans}=1.40 \rightarrow 1.29$ for $Ca=0.2 \rightarrow 5$ as shown in Figure 4. This is very close to 1.31, which describes the flooded feed metering system. That $\lambda_{A,\ trans}$ decreases slightly with increasing Ca>0.1 is in agreement with both Coyle *et al*'s (1986) and Benjamin's (1994) predictions for the metering regime and the transition regime respectively. More interestingly that a turn down in $\lambda_{A,\ trans}$ was predicted by Benjamin's (1994) when $Ca \rightarrow 0$ is also reproduced in our data. It does suggest that there is a maximum $\lambda_{A,\ trans,\ max}$. Considering the experimental difficulties in pinpointing precisely the transition boundary, the agreement between this data and Benjamin's (1994) actual prediction is indeed very good as shown in Figure 4. It is also remarkable that $\lambda_{A,\ trans,\ max} = 1.40$ predicted by Benjamin's (1994) is reproduced in our data. Also, when we compare our data with the prediction of $\lambda_{A,\ trans}=1.34$ at Ca=0.1 given by Carvalho & Scriven (1997), the agreement too is excellent.

As for the values of $(X_D/H_0)_{trans}$ , they vary very much with Ca and are in the range $80 \rightarrow 15$ when $Ca= 0.1 \rightarrow 5$. When we compare our $(X_D/H_0)_{trans}$ data with the prediction of $(X_D/H_0)_{trans}$ at $\lambda_{A,\ trans}=1.34$ at Ca=0.1 by Carvalho & Scriven (1997), we find their two turning points #2 and #3 give 17 and 13 respectively or an average of 15. Our data shown in Figure 5b for the lowest Ca range give similar results. The important observation is that just before dynamic failure, $(X_D/H_0)_{trans}$ still remained located away from the minimum gap position. This explains why we also observed up to the transition boundary that the dynamic wetting line failed by adopting a

vvv-type shape prior to air entrainment. Therefore the plunging flow also describes well dynamic wetting in the rolling bank or at the transition metering regime / pre-metered regime.

**3.3 Pre-metered Regime**: Whilst keeping $H_A/H_0$ not much >1, we could move past the transition condition into the pre-metered regime by reducing the feed flow $Q_A$ further corresponding to $\lambda_A<\lambda_{A,\ trans}$. The accumulation (rolling bank) we observed reduced in size accordingly, the meniscus no longer bulged out and as the metering roller speed was increased, $X_D$ moved right near the minimum gap position until at a critical metering roller speed $V^{**}_M$ the coating bead broke catastrophically, i.e. air was engulfed (cascade) just as observed in reverse roll coating by Coyle *et al.* (1990) and Benkreira (2001). Indeed a quantitative similarity with reverse roll coating can also be drawn when we correlate the data. We find with a confidence limit of ± 12% that:

$$\mathbf{Ca^{**}_M} = (0.63\ (H_A/H_O)^{1.56})\ \mathbf{Ca_A^{0.65}} \qquad (3.1)$$

This is very similar to Equations (1.4) and (1.5) of Coyle *et al.* (1990) and Benkreira (2001).

We could enter the pre-metered regime directly starting with $H_A/H_0$ <1. For the range of Ca tested we could start from $H_A/H_0$ as low as 0.6. For these conditions, the meniscus was firmly streamlined with $X_D$ in the nip and it too broke catastrophically (cascade) at a critical metering roller speed $V^{**}_M$ corresponding to a minimum flow rate $\lambda_{A,\ min}$. The $V^{**}_M$ data for these conditions also conform to the analogy with reverse roll coating (Equation 3.1 above). Therefore the plunging flow is not an appropriate description of dynamic wetting in the pre-metered regime. Figure 4 shows the lowest flow rate $\lambda_{A,\ min}$ is in the range 1.2 $\rightarrow$1.18 when Ca=0.2 $\rightarrow$ 4, exactly as predicted by Benjamin (1994) and Carvalho & Scriven (1997). For the latter we can only make the comparison for the one Ca value given ($\lambda_{A,\ min}$ =1.22 when Ca=0.1). Also the turn down

in $\lambda_{A,\,min}$ at Ca~0 leading to meniscus coating, predicted by Benjamin (1994) is reproduced in the data.

As for the values of $(X_D/H_0)_{min}$ , the essential information is that they are all equal and close to the zero position as shown in Figure 4, which justifies the onset of cascade. The actual data gave $(X_D/H_0)_{min}$=-5 which sets the experimental error in our measurements. It must be pointed that the $(X_D/H_0)_{min}$=-5 line measured was at a metering speed about 0.1 m/min less than the critical speed. The variation of $(X_D/H_0)$ with Ca and $\lambda_A$ is given in Figure 5a,b and compared with the prediction of Benjamin (1994). There is a good qualitative agreement in that in the range Ca=1$\rightarrow$10, $X_D/H_0$ varies essentially with $\lambda_A$ only (Figure 5a) whereas in the range Ca=0.5$\rightarrow$1, $X_D/H_0$ varies with both Ca and $\lambda_A$ (Figure 5b). Quantitatively, there is however a significant discrepancy between the data and predictions which cannot be attributed to experimental errors only since the $X_D$ data at cascade were all located near the expected zero position. As pointed out in the introduction, in the theoretical treatment the dynamic wetting region is difficult to handle and the assumptions made on the contact angle $\theta_D$, slip length and non-hydrodynamic effects will affect the predictions.

**3.4 On Air Entrainment, Cascade and Hydrodynamic assistance**: The observations made above leads to the conclusion that the critical line for forward roll coating is the transition line $\lambda_{A,\,trans} \cong$1.40 to 1.29 as Ca is increased from 0.2 to 5. It divides the dynamic wetting failure from the vvv-type when $\lambda_A > \lambda_{A,\,trans}$ to the cascade type when $\lambda_A < \lambda_{A,\,trans}$. Figure 6, which normalizes all the data in the range $\lambda_A > \lambda_{A,\,trans}$ down to $\lambda_{A,\,min}$ reproduces very well this division. It is interesting to note that for a very small range of $\lambda_A$ [1.32-1.39] both air entrainment and cascade

can occur, with cascade following air entrainment. This may be an important observation when assessing further the physics of these two types of dynamic failure.

Figure 7 shows that the vvv-type dynamic failure speeds $V^*_M$ measured in roll coating are identical to those $V^*_{plunging}$ measured in plunging tape experiments. Our first conclusion is that there is no hydrodynamic assistance in roll coating flows when $\lambda_A > \lambda_{A,\,trans}$ which corresponds to operation in the metering regime up to the metering / pre-metered boundary.

When $\lambda_A < \lambda_{A,\,trans}$ , i.e. when dynamic failure occurs by cascade, the corresponding $V^{**}_M$ can be lower or higher than $V^*_{plunging}$. The data plotted in terms of $Q_A$ vs $V^{**}_M$ as in Figure 8 show a similarity with curtain coating. Unlike $V^*_{plunging}$ which is constant (depends only on viscosity), $V^{**}_M$ depends on $Q_A$ and increases with it up to a maximum value, $V^{**}_{M,\,max}$. In other words increasing $Q_A$ assists wetting up to a maximum speed. The similarity with curtain coating can be taken further. When we process the data of $V^{**}_{M,\,max}$ , we find they correlate with operating conditions with a confidence limit of ±3 to ± 1 to % respectively in the form:

$$\mathbf{V^{**}_{M,\,max}} = (0.203\, H_0^{-1.39}\, H_A^{1.33})\, \mathbf{V_A^{0.81}}\, \boldsymbol{\mu}^{\mathbf{-0.19}} \qquad (3.2a)$$

$$\mathbf{V^{**}_{M,\,max}} = (0.123\, H_0^{-1.05}\, H_A^{0.92})\, \mathbf{V_A^{0.66}}\, \boldsymbol{\mu}^{\mathbf{-0.17}} \qquad (3.2b)$$

These correlations are remarkably very similar to Blake *et al.* (1994) theoretical and experimental equations (1.2) and (1.3) above. This confirms the similarity of hydrodynamic assistance in the two flows. Part of the applicator roll flow is the equivalent of the impinging curtain flow. In comparison however with curtain coating, $V^{**}_{M,\,max}$ observed in forward roll coating is much smaller. This is because the fluid in the gap splits and turn, the impinging component of the applicator roll speed vector is small compared with the curtain speed. Also the converging-diverging geometry of the nip breaks the continuity in the increase of the contact angle when $X_D \rightarrow 0$, resulting in the destabilization of the dynamic wetting line and the subsequent air

engulfment. Also in Figure 8, a careful examination of the data shows at $V^{**}_{M,\,max}$ corresponding to a critical flow rate $Q_{A,\,crit,}$ a further small incremental increase in the flow rate results with a switch back to the vvv-type air entrainment. Effectively at this turning point, air entrainment and cascade occur at the same conditions or $V^{**}_{M,\,max} = V^{*}_{M,\,max}$. When the data corresponding to this switch are picked, they correlate numerically as:

$$\lambda^{*}_{A} = (Q_A / Q_D)^{*} \equiv V_A H_A /1/2\,(V_A + V^{*}_{M,\,max})\,H_0 = 1.27 \qquad (3.3)$$

Therefore there is only a very small range of $\lambda_A$[1.27-1.31], where $V^{*}_{M} > V^{*}_{plunge}$, i.e. practically hydrodynamic assistance is negligible in forward roll coating. It is however present but, because of the converging-diverging geometry, it is prematurely limited by cascade.

## 4. CONCLUSIONS

This experimental study of forward roll coating has been carried out in the practical range of Ca=0.2→5 and established $\lambda_{A,\,trans}$, the transition metering / pre-metered dimensionless applicator flow rate and $\lambda_{A,\,min}$ the minimum pre-metered regime dimensionless applicator flow rate. Both were found to vary little with Ca and were in the range $\lambda_{A,\,trans}$=1.40→1.29 and $\lambda_{A,\,min}$=1.20→1.18. These values compare very well with theoretical predictions. Data from $\lambda_A > \lambda_{A,\,trans}$ down to $\lambda_{A,\,min}$ were also presented for the variation of the dimensionless dynamic wetting line position $X_D/H_0$ with Ca up to the onset of air entrainment or cascade. The measured $X_D/H_0$ agree qualitatively but differ significantly from theoretical predictions and this suggests that the current theoretical treatment of the dynamic wetting region in forward roll coating needs re-examining. It was found $\lambda_A$ is the key parameter as it defines the flow regimes and whether dynamic failure occurs by air entrainment or cascade. For $\lambda_A \geq \lambda_{A,\,trans}$, dynamic failure occurs by

air entrainment similar to plunging tape flow and at identical speeds, which depends on viscosity only. For $\lambda_A<\lambda_{A,\ trans}$, dynamic failure occurs by cascade similar to reverse roll coating. These cascade speeds depend on $\lambda_A$ as well as viscosity and can be smaller or larger than the corresponding air entrainment plunging tape speed. A maximum speed $V^{**}_{M,\ max}$ occurs at $\lambda_A$=1.27 when cascade switches to become air entrainment. The study draws analogies with hydrodynamic assistance in curtain coating and cascade in reverse roll coating both of which are supported by the data.

**Acknowledgements**

The author acknowledges the financial support of The UK Research Council under EPSRC grant, GR/L96493. The data reported here were collected by Dr R.Patel who was the post-doctoral assistant employed in this project.

**NOTATION**

| | |
|---|---|
| Ca, $Ca_A$, $Ca_M$ | capillary number ($0.5(V_A+ V_S)\ \mu/\sigma$, $\mu V_A/\sigma$, $\mu V_M/\sigma$,) |
| $H_0$, $H_A$ | metering gap, applicator film thickness (m) |
| $Q_A$, $Q_N$, $Q_D$ | applicator, net, drag flow ($m^3/s$) |
| $U_i$ | impingement speed in curtain coating flow (m/s) |
| $V_S$ (=$V_M$) | substrate speed (m/s) |
| $V_A$ , $V_M$ | applicator, metering roll speed (m/s) |
| $V^*$ | air entrainment speed (m/s) |
| $V^{**}$ | cascade speed (m/s) |
| $X_D$ | dynamic wetting line position (m) |
| $\lambda_A$, $\lambda_N$ | dimensionless applicator, net flow |

$X_D/ H_0$ dimensionless dynamic wetting line position

$\theta_S$ , $\theta_D$ static and dynamic contact angle ($^0$)

$\mu$, $\rho$, $\sigma$ fluid viscosity (Pa.s), density (kg/m$^3$), surface tension (kg/s$^2$)

**REFERENCES**


1. Benjamin D.F. (1994) Roll coating flows and multiple flows systems. PhD Thesis, University of Minnesota, Minneapolis.
2. Benkreira, H. (2001) An experimental study of dynamic wetting in reverse roll coating. *A.I.ChE. J.*, ,.
3. Benkreira, H., Edwards, M.F. & Wilkinson, W.L. (1981) Roll coating of purely viscous fluids. *Chem. Eng. Sci*., **36**, 429.
4. Benkreira, H., Edwards, M.F. & Wilkinson, W.L. (1981) A semi-empirical model of the forward roll coating flow of Newtonian fluids. *Chem. Eng. Sci*., **36**, 423.
5. Blake, T.D., Clarke A. & Ruschak, K.J. (1994) Hydrodynamic assist of dynamic wetting. *A.I.ChE. J*., **40**, 229.
6. Blake, T.D. & Ruschak, K.J. (1979) A maximum speed of wetting. *Nature*, **282**, 489.
7. Burley, R. & Kennedy, B.S. (1976) An experimental study of air entrainment at a solid-liquid-gas interface. *Chem. Eng. Sci*., **31**, 901.
8. Burley, R. (1992) Mechanisms and mechanics of air entrainment in coating processes. *Industrial Coating Research*, **2**, 95.
9. Buonoplane, R.A., Gutoff E.B. & Rimore M.M.T. (1986) Effect of plunging tape surface properties on air entrainment velocity. *A.I.Ch.E. J*., **32**, 682-683.
10. Carvalho, M.S. & Scriven, L.E. (1997) Multiple states of a viscous free surface

flow: Transition from pre-metered to a metering inflow. *Int. J. Numer. Methods Fluids*, **24**, 813.

11. Chen, K.S.A. & Higgins, B.G. (1988) Study of the flow in the upstream bank of liquid in a forward roll coater by the finite element method. *Chem. Eng. Sci*., **43**, 2867.
12. Cohu, O., & Benkreira, H. (1998) Air entrainment in angled dip coating. *Chem. Eng. Sci*., **53**, 533.
13. Coyle, D.J., Macosko, C.W. & Scriven, L.E. (1986) Film splitting flows in forward roll coating. *J. Fluid Mech.*, **171**, 183.
14. Coyle, D.J., Macosko, C.W. & Scriven, L.E. (1990) The fluid dynamics of reverse roll coating. *A.I.Ch.E. J*., **36** (2), 161.
15. Deryagin B.M. & Levi S.M. (1964) Film Coating Theory. Focal Press, London.
16. Gaskell, M.D., Savage, M.D., Summers, J.L. & Thompson, H.M. (1995) Modelling and analysis of meniscus roll coating. *J.Fluid Mech.,* 28, 113.
17. Gutoff E.B. & Kendrick C.E. (1982) Dynamic contact angles, *A.I.Ch.E J*., **28**, 459.
18. Gutoff & Kendrick (1987) The flow limits of coatabilty on a slide Coater. *A.I.ChE. J*., **33**, 141-145.
19. Kistler, S.F. (1983) The Fluid Mechanics of curtain coating and related viscous free surface flows with contact lines. PhD Thesis, University of Minnesota, Minneapolis.
20. Kistler, S.F. & Schweizer. P.M. (eds). (1997) *Liquid Film Coating*. Chapman & Hall, London.
21. Lee, K.Y. & Liu, T.J. (1990) Minimum wet thickness of extrusion slot coating. *A.I.Ch.E Spring Nat. Meet.*, Orlando.
22. Papanastasiou, T.C., Malamataris, N. & Ellwood, K. (1992)) A New Outflow Boundary

Condition. *Int. J.Numer. Methods Fluids*, **14**, 587.

23. Yamamura, M., Suematsu, T., Kajiwara, T. & Adachi, K. (2000) Experimental investigation of air entrainment in a vertical liquid jet flowing down onto a rotating roller.

*Chem. Eng. Sci*., **55**, 931.

**LIST OF FIGURES AND CAPTIONS**

Figure 1: Forward roll coating: geometry and operating parameters.

Figure 2: Flow regimes in forward roll coating: (a) flooded inlet-metering, (b) rolling bank- limit metering / pre-metered, (c) pre-metered ($\lambda_A \sim 1$), (d) meniscus coating ($\lambda_A << 1$)

Figure 3: Experimental set-up: 1-coating pan, 2-steel roller, 3-perspex roller, 4-scraper blade, 5-side viewing window, 6-xyz moveable frame, 7-CCD camera with micro lens, 8-metering blade.

Figure 4: Coating window $\lambda_A = f(X_D/H_0, Ca)$ with limits $\lambda_{A,\,trans}$ for air entrainment and $\lambda_{A,\,min}$ for cascade and comparison with Benjamin's (1994) theory (----).

Figure 5a: Wetting line position function $X_D/H_0 = f(Ca, \lambda_A)$ and comparison with Benjamin (1994). Data: ◊ (Ca=1-4). Predictions: ---(Ca=1), — (Ca=10).

Figure 5b: Wetting line position function $X_D/H_0 = f(Ca, \lambda_A)$ and comparison with Benjamin (1994). Data: X ($\mu$=0.201 Pa.s, Ca=0.5-1), O ($\mu$=0.055 Pa.s, Ca=0.5-1). Predictions: ---(Ca=0.5), — (Ca=1.0).

Figure 6: Normalized data showing dividing effect of $\lambda_A$ on air entrainment ($\Delta$) and cascade (O).

Figure 7: Data (•) for air entrainment speeds $V^*$ at $\lambda_A \geq \lambda_{A,\,trans}$ and comparison with Gutoff and Kendrick (1982) correlation (----): $V^*_{plunging} = 0.05\ \mu^{-0.67}$.

Figure 8: Analogy with curtain coating: effect of applicator flow rate, $Q_A$ on air entrainment speed $V^*_M$ or cascade speed, $V^{**}_M$. Data with $\mu$=204 mPa.s, $H_0$=0.75 mm and $H_F$ = 900 μm (O), 800 μm (P), 700 μm (♦), 600 μm (□), 500 μm (λ). Corresponding $V^*_{plunging}$ =0.145m/s

**KEY PARAMETERS: $H_A/H_o$ , $\lambda_A = Q_A/Q_D$ , $\lambda_N = Q_N/Q_D$**

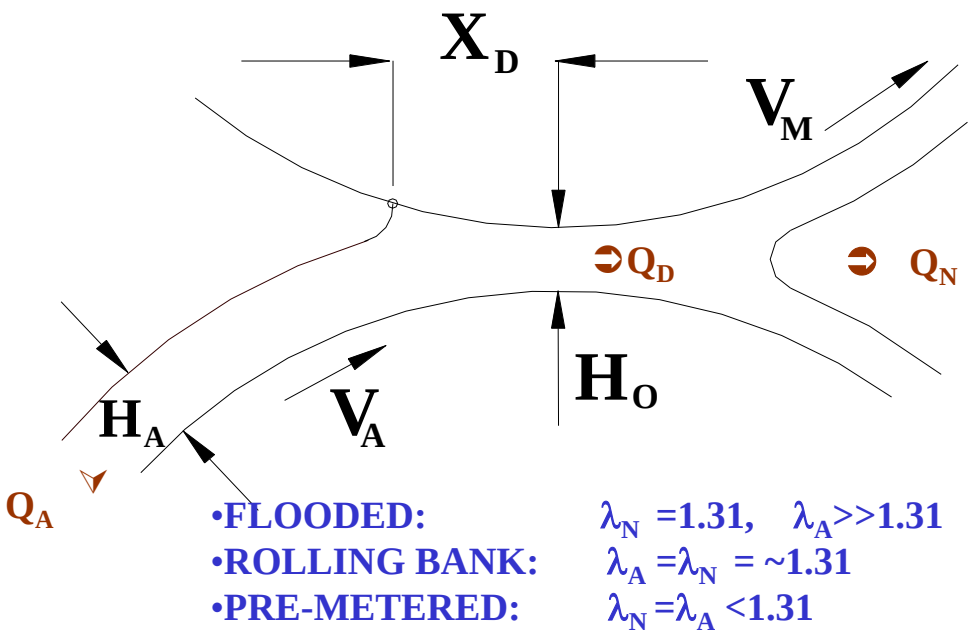


**Ca range 0.1-10, i.e not concerned with meniscus coating, $\lambda_N = \lambda_A << 1$**

**FIGURE 1**

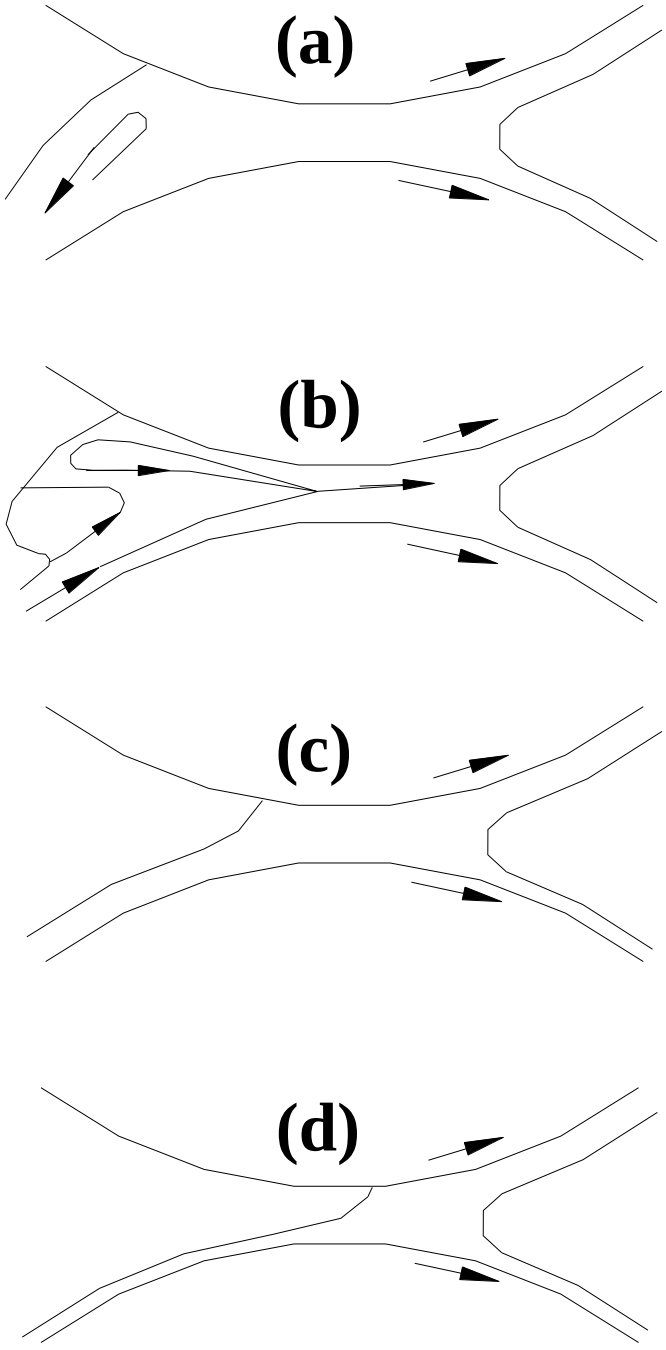


**FIGURE 2**

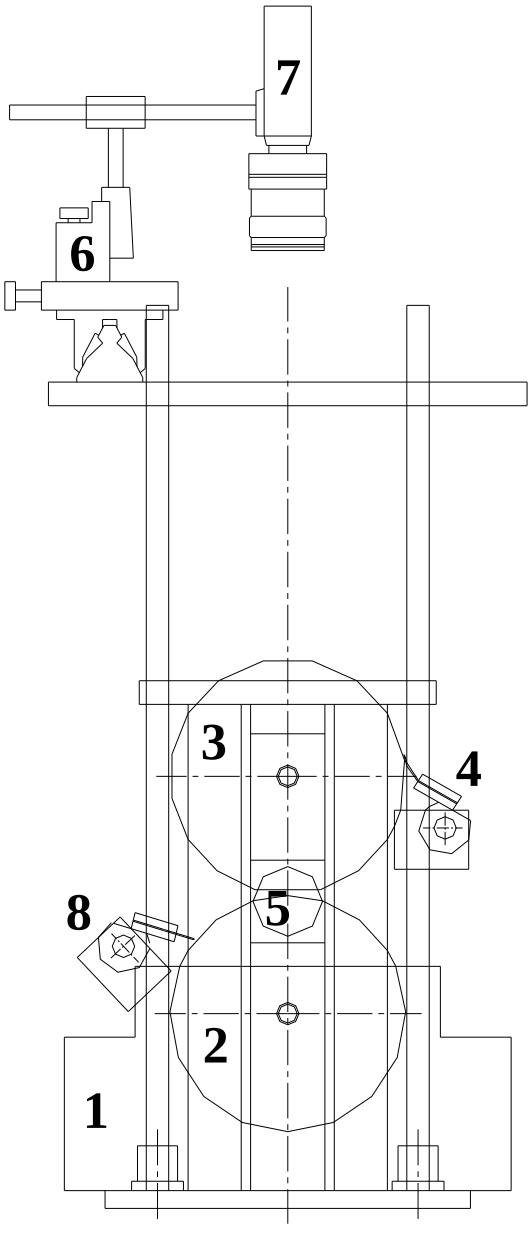


**FIGURE 3**

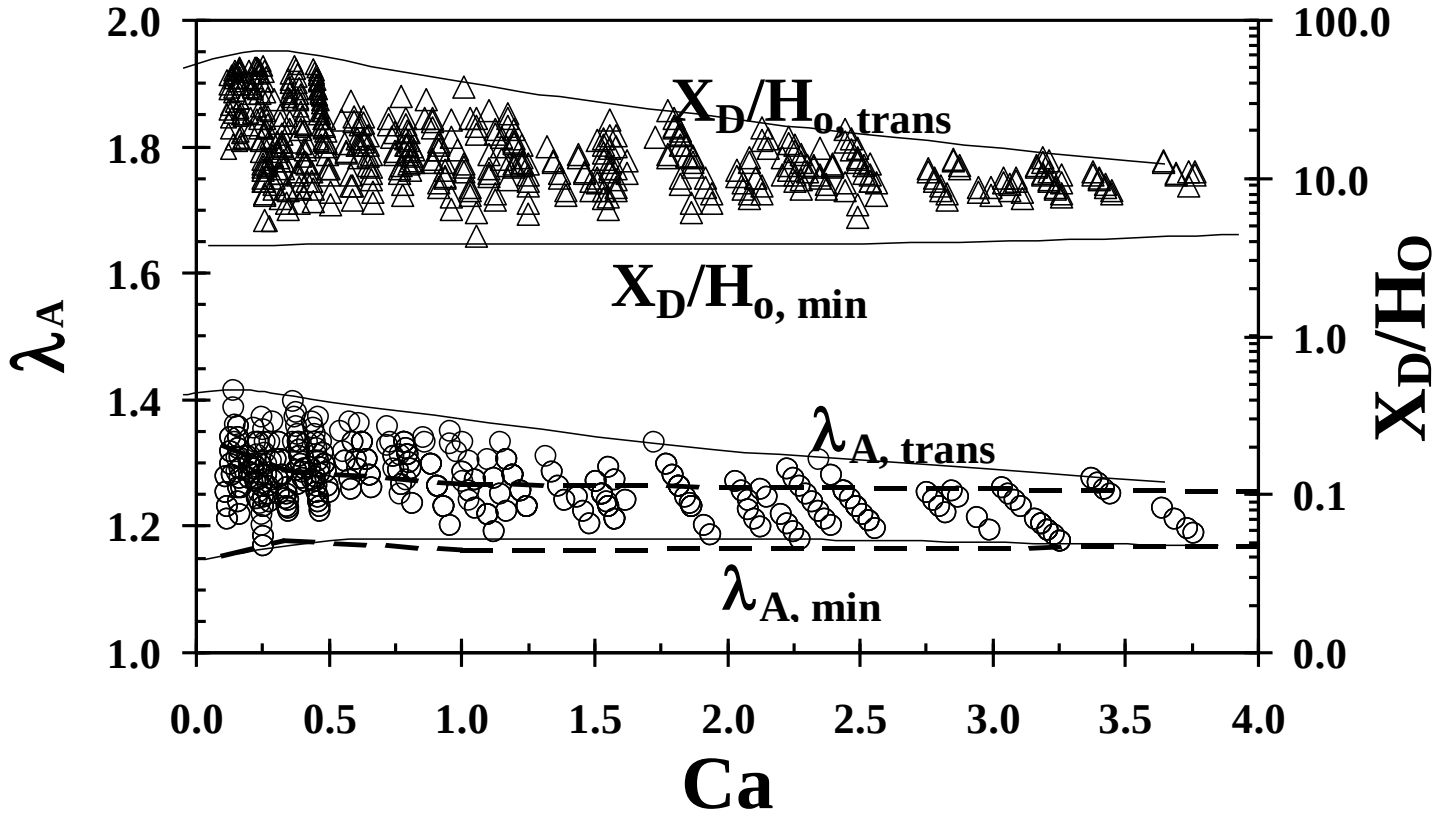
2.0
1.8
1.6
1.4
1.2
1.0
100.0
10.0
1.0
0.1
0.0
$\lambda_A$
$X_D/H_o$
$X_D/H_{o,\ trans}$
$X_D/H_{o,\ min}$
$\lambda_{A,\ trans}$
$\lambda_{A,\ min}$
0.0
0.5
1.0
1.5
2.0
2.5
3.0
3.5
4.0
Ca

**FIGURE 4**

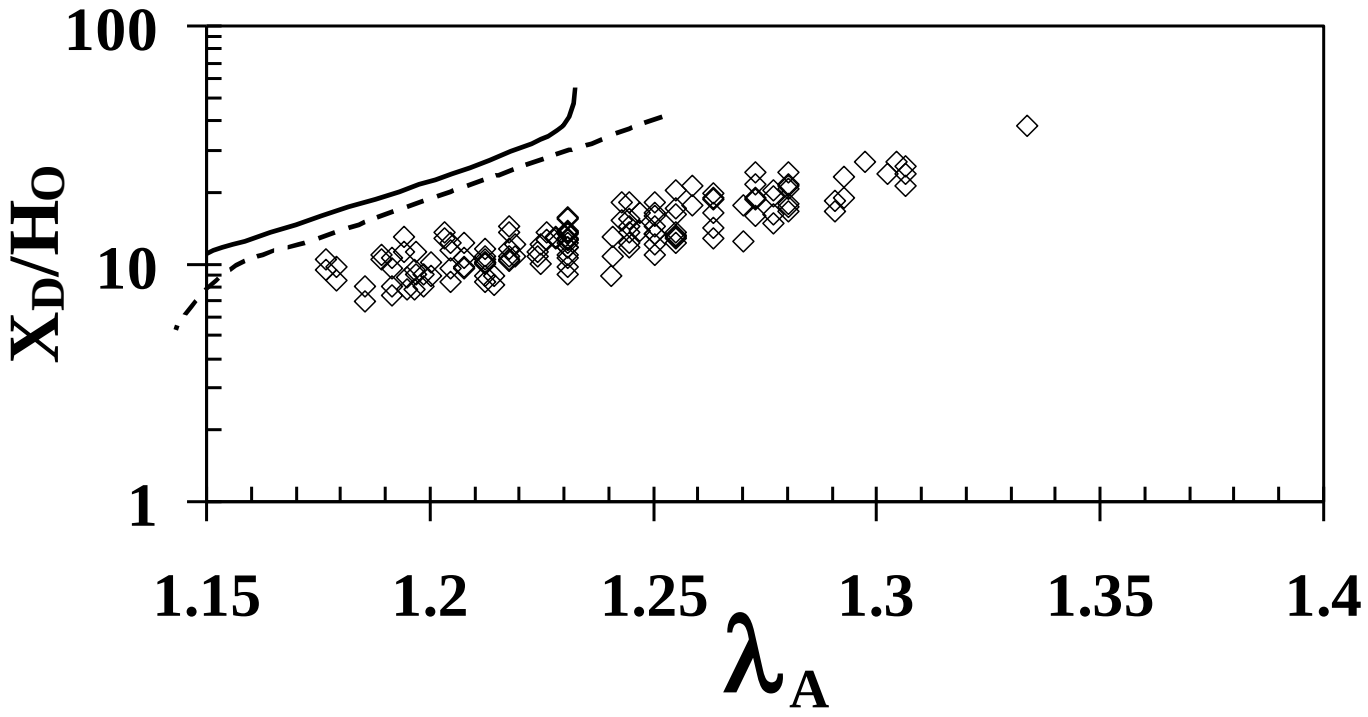


**Figure 5a**

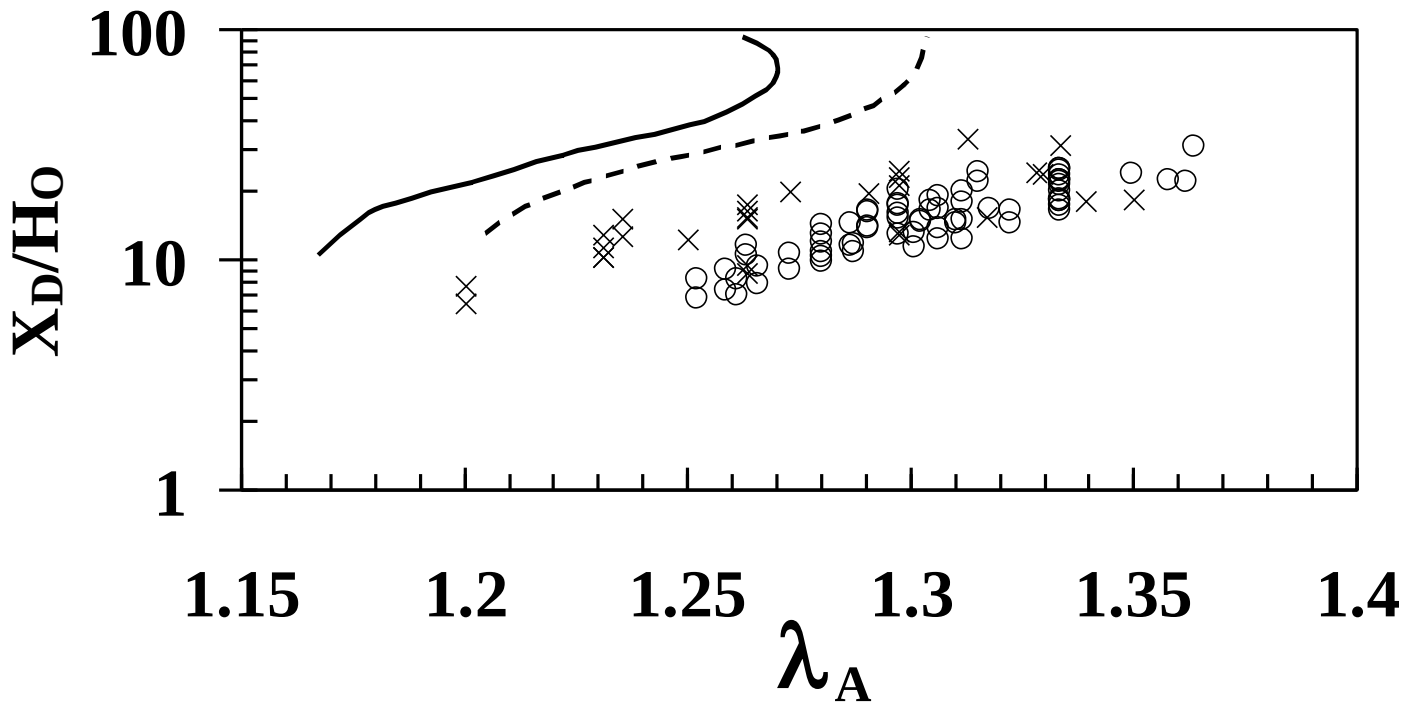


**FIGURE 5b**

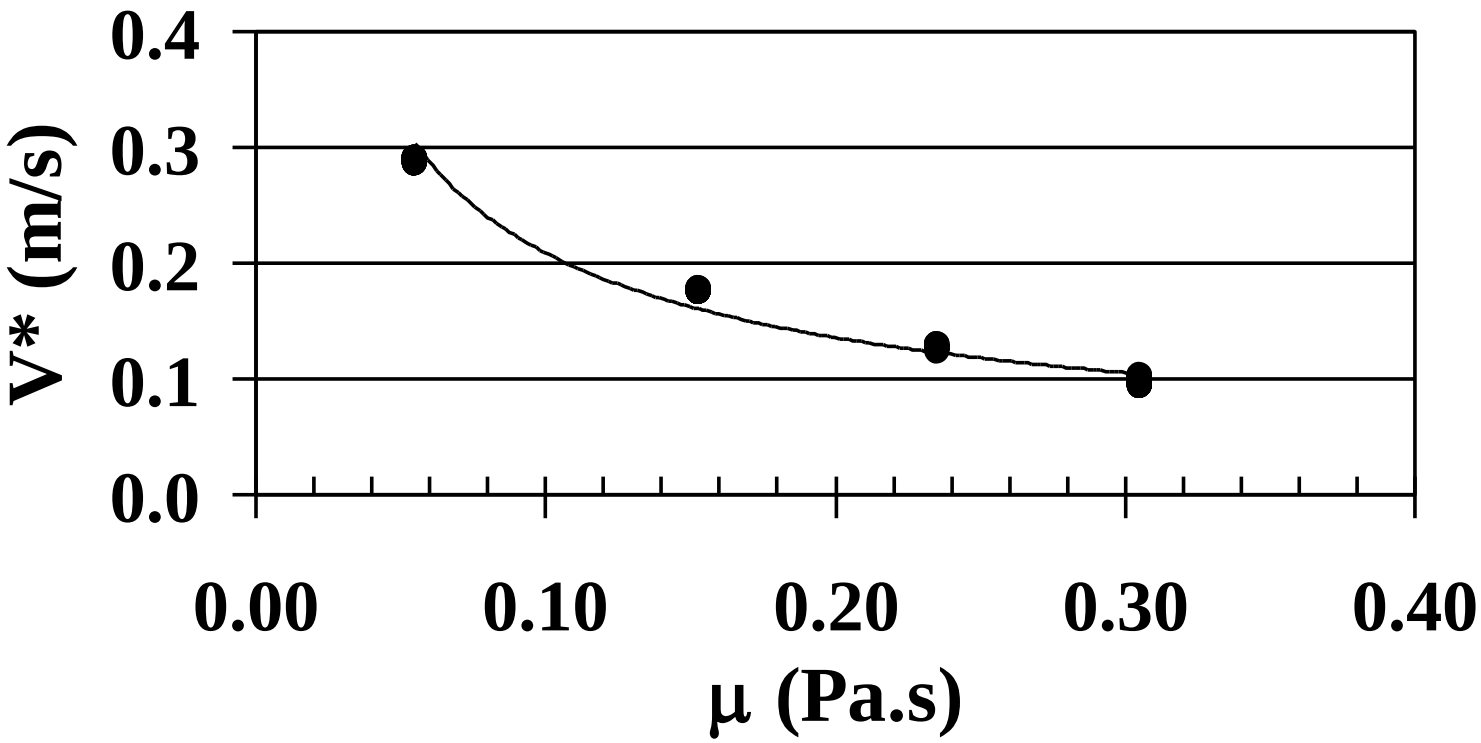


**FIGURE 6**

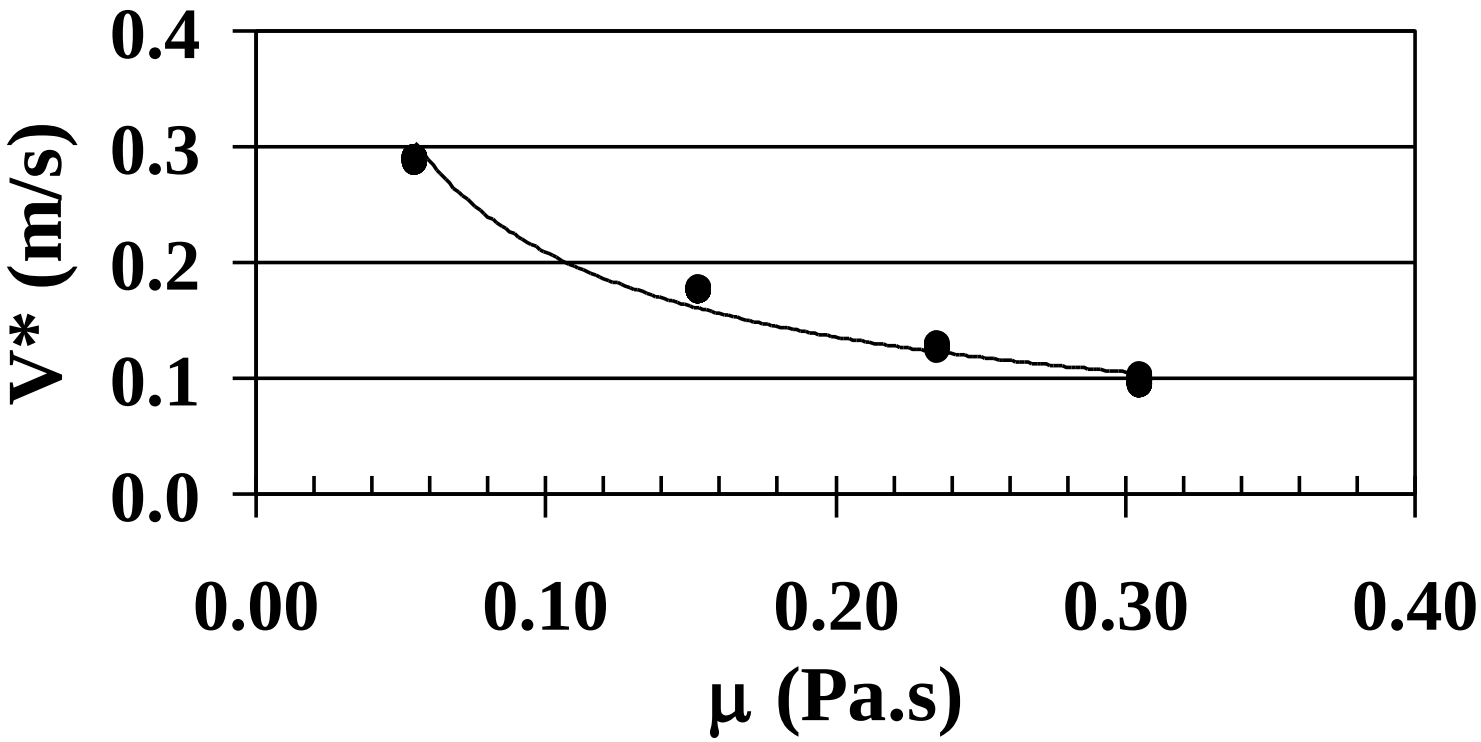


**FIGURE 7**

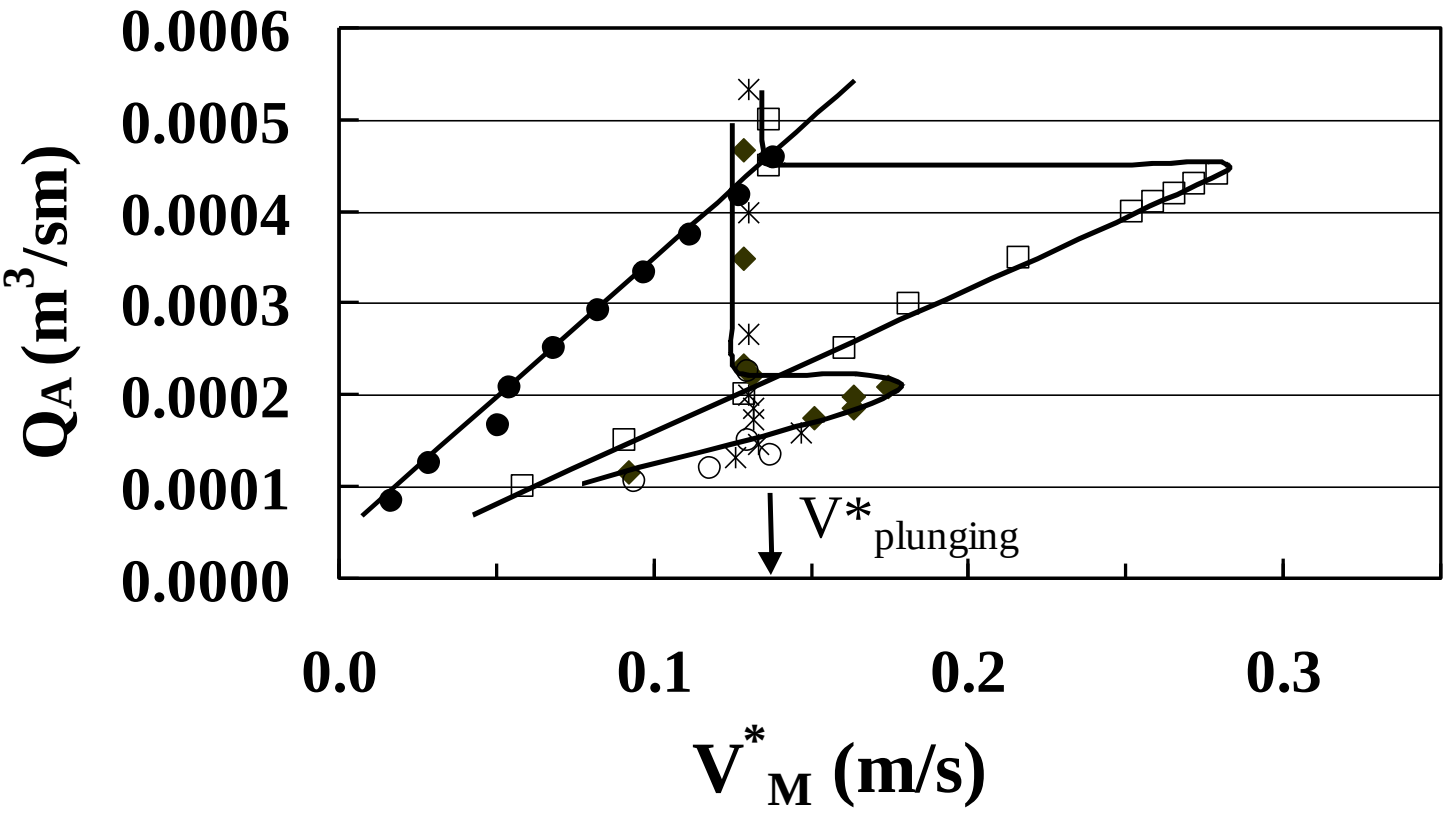
0.0006
0.0005
0.0004
0.0003
0.0002
0.0001
0.0000
$Q_A$ ($m^3$/sm)
V*plunging
0.0
0.1
0.2
0.3
$V^*_M$ (m/s)

**FIGURE 8**